Phenomenological model of shock initiation in heterogeneous explosives

E. L. Lee and C. M. Tarver

Citation: Phys. Fluids **23**, 2362 (1980); doi: 10.1063/1.862940
View online: http://dx.doi.org/10.1063/1.862940
View Table of Contents: http://pof.aip.org/resource/1/PFLDAS/v23/i12
Published by the American Institute of Physics.

Phenomenological model of shock initiation in heterogeneous explosives

E. L. Lee and C. M. Tarver

Lawrence Livermore National Laboratory, Livermore, California 94550
(Received 3 December 1979; accepted 20 August 1980)

An ignition and growth concept is used, within the framework of a one-dimensional Lagrangian hydrodynamic code, to model the shock initiation of heterogeneous solid explosives. The leading shock wave of an initiating pulse is assumed to ignite a small fraction of the explosive at localized heated regions. These ignited regions then grow as material is consumed at their boundaries. The growth rate for a particular material is assumed to have the characteristic pressure dependence of high-pressure laminar burning experiments. Results of the model calculations are in good quantitative agreement with recent manganin pressure gage and particle velocity gage measurements of the buildup of the initiating shock front to detonation for both sustained and short duration pulses in four solid explosives: PBX – 9404, TATB, cast TNT, and PETN. The predicted run distances to detonation as functions of shock pressure at various initial densities and the predicted reaction zone lengths of the fully developed detonation waves also correlate well with experimental data for these four solid explosives.

I. INTRODUCTION

A complete determination of the process by which an impulse delivered to an explosive evolves into a self-sustaining detonation wave, would require not only a complete determination of the macroscopic hydrodynamic flow but also a detailed microscopic measurement of the small scale nucleation and turbulent phenomena. These phenomena must play an important part in heterogeneous materials, if not in all explosive materials. Experimental researchers over the past thirty years have provided progressively more accurate and complete data. During this time, the development of theoretical models to better understand the shock initiation process has often lagged behind the experimental observations. Efforts to extend the models to predict hitherto unobserved results have been very limited.

Since the ignition and growth concept discussed in this paper also makes extensive use of the available experimental data to parameterize the equations and to test the phenomenological models, it is useful to briefly review the experimental evidence and the development of theoretical models of shock initiation in heterogeneous explosives.

A. Development of experimental techniques

It has long been recognized[1] that the shock initiation of heterogeneous explosives is controlled by the formation and subsequent reaction of the hot spots that have been created by various localized heating mechanisms as the shock pulse compressed the heterogeneous solid. The ignition of these "hot spots" is strongly dependent on the constitutive state of the explosive, especially the porosity and the crystalline microstructure. Many excellent experimental studies of shock initiation of heterogeneous explosives at various initial densities have been conducted by determining the trajectory of the shock front and the ensuing detonation wave through a wedge of explosive. Seay and Seely[2] determined the shock initiation threshold of PETN wedges pressed to a density of 1.0 g/cm^3 for sustained pulses from brass and Lucite plates. Ramsay and Popolato[3] reported the measured excess transit times and run distances to detonation versus shock pressure for sustained pulses in wedges of several explosives at higher densities. In later wedge test studies, PETN-based,[4] RDX-based,[5] and tetryl-based[6] explosives were used to determine run distances to detonation versus shock pressure for sustained pulses driving explosives at various initial densities and degrees of porosity.

In addition to these sustained pulse studies, Gittings,[7] and later, Trott and Jung[8] studied the shock initiation of PBX-9404 and Comp B by short duration shock pulses produced by propelling thin aluminum flyer plates into the explosive sample at various velocities and measuring the transit time of the pulse through the sample. These studies yielded critical impact velocity or pressure versus pulse duration curves for initiation of detonation and excess transit time measurements for samples that did detonate.

More recent experimental studies have revealed that in heterogeneous explosives the principal buildup of chemical reaction lies in a region behind the lead shock, and not as closely coupled to the trajectory of the shock front, as had earlier been supposed. Liddiard,[9] using a fast framing camera, reported delayed (6 to 30 μsec) burning reactions when PBX-9404 was subjected to low amplitude (0.5 to 1.5 GPa) shocks in underwater experiments. Green[10] in similar experiments observed delays of 40 to 70 μsec before burning reactions began in PBX-9404 subjected to even lower amplitude (0.3 to 0.5 GPa) shocks in underwater tests. Using a free surface velocity technique, Craig and Marshall[11] reported significant decomposition behind the shock front as well as partial reaction at the front in shocked but not detonated PBX-9404 for initial shock pressures in the 2.3 to 5.8-GPa range. Kennedy[12,13] used a quartz guage technique to observe pressure buildup behind the shock front when the initial stress into PBX-9404 exceeded 3.0 GPa. With a laser interferomatic technique, Kennedy and Nunziato[14] measured the increase in particle velocity behind the shock front in PBX-9404 for two pulse durations at an intial stress level of approximately 3.7 GPa.

 0031-9171/80/122362-11$00.90

Important recent developments in experimental shock initiation research have been the perfection of thin embedded manganin pressure gages and embedded particle velocity gages. These techniques allow detailed, quantitative studies of the flow fields in the region of buildup to detonation in one-dimension shock initiation experiments. Cowperthwaite and Rosenberg[15] measured the hydrodynamic flow behind the shock front in cast TNT shocked to about 5.5 GPa with Dremin loop particle velocity gages and developed a direct analysis of Lagrange gage data to interpret these data in terms of reaction rates. Manganin pressure-gage records of the pressure histories at several gage planes in the buildup region for relatively high input shock pressures (>2 GPa) and short run distances to detonation (<20 mm) have been obtained in four heterogeneous solid explosives: PETN,[16] TNT (cast[17,18] at a density of 1.61 g/cm^3 and pressed[19] to a density of 1.56 g/cm^3), TATB,[20] and PBX-9404.[20,21] Both sustained and short pulse durations have been used to obtain manganin gage data in cast TNT[18] and PBX-9404.[21] Recently, Green, *et al.*[22] studied the reaction buildup in PBX-9404 from low amplitude (0.4–1.4 GPa), long-duration shock pulses in 102-mm long specimens containing multiple embedded manganin gages.

These pressure and particle velocity measurements have greatly increased the knowledge of the buildup to detonation region in the one-dimensional shock initiation of solid explosives. These measurements clearly show that the initial shock front increases slowly in amplitude as it propagates through the explosive. However, they provide strong evidence that the principal pressure buildup occurs behind the leading shock front, and the transition to detonation occurs very rapidly as the trailing pressure pulse overtakes the leading shock front.

B. Development of the theoretical models

The development of the theoretical understanding of shock initiation of heterogeneous explosives has closely paralleled the experimental progress. The "hot spot" concept, originally proposed by Bowden[23] and Eyring,[24] postulated a grain burning mechanism for the propagation of detonation. Hubbard and Johnson[25] pioneered the use of one-dimensional hydrodynamic computer codes to model shock initiation using Arrhenius kinetics. Mader[26,27] extended the use of Arrhenius kinetics to studies of the formation of hot spots by void closure and the subsequent thermal explosion of hot spots. Boyer[28] used a reaction rate model that included the hot spot, grain burning, and diffusion controlled reaction concepts and was able to fit shock trajectory data for shock initiation of TNT. Hydrodynamic calculations by Enig and Petrone[29,30] showed the importance of the temperature variation in the equation of state of the unreacted explosive in initiation calculations involving Arrhenius kinetics. In fact, the problems of calculating[31] (much less measuring) the temperature of a shocked explosive for use in an Arrhenius kinetic reaction rate equation still severely limit the usefulness of such calculations.

In the analysis of short pulse duration shock initiation data for TNT, Walker and Wasley[32] proposed a critical energy criterion for initiation of detonation which has become known as the $p^2\tau = \text{const}$ criterion. This rather simple criterion has been the subject of considerable experimental work and theoretical discussion.[33] de Longueville *et al.*[34] in an extensive study of granular, pressed, cast, and liquid explosives showed that the $p^2\tau$ or constant critical energy concept describes initiation behavior over wide ranges of pressure and pulse duration for PBX-9404 and Comp B, but does not correlate with shock initiation data on liquid TNT, nitromethane, and some RDX-based explosives. As it was originally intended, the $P^2\tau$, or critical energy criterion, has been shown to be a very useful engineering tool for predicting shock initiation of certain explosives over certain ranges of pressure and pulse duration.

This brief summary illustrates the variety of empirical and phenomenological models which have been applied to the shock initiation problem. Within carefully defined limits, these models has successfully simulated experimental results. The use of a pressure-dependent reaction rate law rather than one based on Arrhenius kinetics in a one-dimensional hydrodynamic calculations was first reported by Bernier *et al.*[35] Using run distance to detonation versus shock pressure data as input to the reaction rate equation, Mader and Forest[36] developed a semiempirical shock initiation model, based on the dependence of detonation delay time on shock pressure that has been applied to two-dimensional detonation wave propagation in homogeneous and heterogeneous explosives[37] and to shock initiation of heterogeneous explosives at various initial densities.[38]

Recent theoretical modeling efforts have attempted to reconcile the type of reaction rate implied by the Lagrange gage experiments previously described. Using manganin gage data from PBX-9404[20] as a basis for similarity solutions, Cowperthwaite[39] constructed solutions that qualitatively describe the hydrodynamic flow and that indicate a two-step energy release rate. A continuum model for hot-spot initiation of granular explosives formulated by Nunziato *et al.*[40] matched the qualitative features of the early shock growth observed by the laser interferometric technique in PBX-9404.[14] Wackerle *et al.*[21] successfully reproduced their sustained and thin pulse pressure histories in PBX-9404 with a reaction rate law containing a quadratic pressure term, an Arrhenius kinetics term, and an induction time factor based on the plastic work at void peripheries being proportional to $\int p^2\,dt$ and on a pressure cutoff for reaction of 0.75 GPa. Using the direct analysis[15] of gage data, Kamel and Dremin[17,18] have employed a pressure-dependent reaction rate law that agrees reasonably well with the early part of their pressure gage data.

In this paper, a phenomenological model is developed which applies to a wide range of materials and a wide range of shock initiation stimuli. An earlier version[41] of the ignition and growth model presented in this paper was used to calculate initiation in PBX-9404[22] from low amplitude shock waves and to demonstrate the significant difference in shock initiation behavior of PBX-9404 below 1.4 GPa as compared with the initiation be-

havior above 2.0 GPa.[3,14,20,21] In this paper, the ignition and growth approach to modeling the one-dimensional shock initiation of heterogeneous explosives is described in detail, and results are presented to show that quantitative agreement can be achieved with the pressure-time, particle velocity-time, and run distance to detonation data for varying stimuli over the wide range of behavior exhibited by the four solid explosives for which detailed experimental data have been published.

II. THE IGNITION AND GROWTH MODEL

A. General discussion of ignition and growth

The ignition and growth concept of shock initiation in heterogeneous explosives was incorporated into a special version of the one-dimensional Lagrangian hydrodynamic code KOVEC.[42] This version was designed to yield stable detonation waves based on the Zeldovich–von Neumann–Doring model.[43] Detonation waves thus consist of a leading shock front in which little or no chemical reaction occurs followed by a well-defined reaction zone in which the pressure decreases to the Chapman–Jouguet value as the fraction of explosive reacted approaches one. The fraction of explosive reacting per cycle is limited to insure precise resolution of the reaction zone and reliable evaluation of the energy and pressure. The volumes of the unreacted explosive and its reaction products are assumed to be additive, and pressures are assumed to be in equilibrium. This work assumes a heterogeneous process in which the temperatures of the reacted and unreacted material are not in equilibrium.

The Jones–Wilkins–Lee equation of state[44] was used in the ignition and growth calculations for both the unreacted explosives and their reaction products. This equation of state has the form

$$p = A\left(1 - \frac{w}{R_1 V}\right)\exp(-R_1 V) + B\left(1 - \frac{w}{R_2 V}\right)\exp(-R_2 V) + \frac{wE}{V}, \tag{1}$$

where p is pressure in megabars, V is the volume of the material at pressure p divided by the initial volume of the unreacted explosive, E is the internal energy and A, B, R_1, R_2, and w are adjustable constants. For unreacted explosives, the constant B is negative allowing the solid to undergo tension and w is set equal to the initial Gruneisen coefficient. This equation of state is fitted to initial sound velocity and experimental Hugoniot data, and the initial internal energy is adjusted to fix $p = 0$ when $V = 1$ at the initial temperature (generally 298°K). This form has some advantages over forms based on a linear shock velocity-particle velocity fit to Hugoniot data. The Jones–Wilkins–Lee equation of state can accommodate the measured bulk sound velocity and the experimentally observed curvature of shock velocity–particle velocity relationship at low shock pressures, while still approaching the linear shock velocity–particle velocity data at higher shock pressures. Table I contains the unreacted equation of state parameters and the resulting calculated von Neumann spike conditions for the four solid explosives examined in this paper, The equation of state parameters and the Chapman–Jouguet state for the reaction products are derived primarily from fits to the experimental cylinder test expansion data for these explosives[45] and are listed in Table II.

The chemical energy release rate laws in the ignition and growth models are based on considerable experimental evidence that the ignition of the explosive occurs in localized hot spots and that the buildup to detonation occurs as the reaction grows outward from these reaction sites. As shown by Taylor and Ervin,[46] the ignition and buildup sensitivities to shock can be separated. The formation of hot spots can be explained by several plausible mechanisms (void closure, microjetting in collapsing voids, plastic work at void peripheries, friction between particles, etc.). Von Holle[47] recently reported the first actual measurements of hot-spot temperatures in shocked PBX-9404 using a time resolved infrared radiometric technique. His results indicated relatively small amounts of material ignited close to the shock front in agreement with the predictions of the model presented here.

The growth of chemical energy release from these hot spots has been the subject of a great deal of research, as reviewed by Howe *et al.*[48] Generally, the growth has been treated as a thermal explosion mechanism or by a grain burning mechanism in which the

TABLE I. Equation of state parameters for unreacted explosives.

Explosives	PBX-9404	TATB(RX-03-BB)	PETN	Cast TNT
ρ_0(g/cm^3)	1.842	1.90	1.75	1.61
w	0.8578	1.251	1.173	0.8926
A(Mbars)	69.69	108.2	37.46	17.98
B(Mbar)	−1.727	−2.406	−1.313	−0.931
R_1	7.8	8.2	7.2	6.2
R_2	3.9	4.1	3.6	3.1
Cv(Mbars/°K)	2.505×10^{-5}	2.724×10^{-5}	2.263×10^{-5}	2.050×10^{-5}
		von Neumann spike conditions		
D(mm/μsec)	8.80	7.596	8.21	6.845
P_s(Mbars)	0.563	0.355	0.452	0.281
V_s/V_0	0.6057	0.6757	0.6068	0.6285
u_s(mm/μsec)	3.470	2.460	3.188	2.5466

TABLE II. Equation of state parameters for reaction products.

Explosive	PBX-9404	TATB	PETN	Cast TNT
E(Mbars-cc/cc)	0.102	0.069	0.101	0.070
A(Mbars)	8.524	6.5467	6.17	3.712
B(Mbars)	0.1802	0.071 236	0.169 26	0.032 306
R_1	4.6	4.45	4.4	4.15
R_2	1.3	1.2	1.2	0.95
w	0.38	0.35	0.25	0.30
Cv(Mbars/°K)	1×10^{-5}	1×10^{-5}	1×10^{-5}	1×10^{-5}
	Chapman–Jouguet conditions			
P_{CJ} (Mbars)	0.370	0.275	0.335	0.210
V_{CJ}/V_0	0.7403	0.7492	0.7253	0.7317
u_{CJ}(mm/μsec)	2.29	1.91	2.28	1.84

intergranular surface area controls the rate of reaction.

In the ignition and growth model described in this paper, a small fraction of the explosive is assumed to be ignited by the passage of the shock front, and the reaction rate is controlled by the pressure and the surface area as in a deflagration process. The explosive material can be consumed very rapidly since the number of hot spots can be very large. Micron-sized spherically burning regions grow and interact to consume the intervening material within microseconds in most cases. The most physically justifiable models have produced the best simulations of the experimental results. They can be represented by the generalized energy release rate equation

$$\frac{\partial F}{\partial t} = I(1-F)^x \eta^r + G(1-F)^x F^y p^z , \tag{2}$$

$$\eta = V_0/V_1 - 1 , \tag{3}$$

where F is the fraction of explosive that has reacted, t is time, V_0 is the initial specific volume of the explosive, V_1 is the specific volume of the shocked, unreacted explosive, p is pressure in megabars, and I, x, r, G, y, and z are constants.

B. Hot-spot formation and ignition concepts

The rate equation was used to investigate several concepts of hot spot formation and subsequent growth of reaction from these hot spots. The η^r term in Eq. (2) was used to investigate various hot-spot formation concepts, because η, the relative compression of the unreacted explosive, can be related through the unreacted equation of state to any of the thermodynamic parameters that may be involved in the initiation process. To a good approximation, p is proportional to η^2 and the square of the particle velocity u_p^2 is proportional to η^3 over the range of compressions and pressures of interest in shock initiation.

In the first reported application of the ignition and growth model to the shock initiation experiments in PBX-9404,[22] the reaction rate equation

$$\frac{\partial F}{\partial t} = I(1-F)^{2/3}\left|\frac{\partial \ln V_1}{\partial t}\right| + G(1-F)^{2/3}F^{2/3}p^{1.2} , \tag{4}$$

included an ignition rate which was simply proportional to the strain rate in the shocked explosive. When integrated over the time required for shock compression, the fraction of explosive ignited is proportional to η, and Eq. (2) with $r=1$ yields the same results as Eq. (4). Subsequent applications of this ignition rate showed that this formulation did not apply over an extended range of stimuli or material properties.

One model of hot-spot formation postulates that hot spots are formed during the stagnation of microjets of material accelerated into rapidly closing voids as the shock front propagates over the irregular particles and voids of a granular explosive. The energy deposited in these hot spots is proportional to the square of the particle velocity in the shocked explosive. The stagnation of accelerated material as an ignition mechanism was first postulated by Seely[49] and later elaborated on by Stresau and Kennedy.[50] The shock initiation data of Roth[51] supports their idea of a critical particle velocity immediately behind the shock front which was nearly independent of loading density for four explosives. In order to investigate this ignition concept, Eq. (2) with $r=3$ is used, since the square of the particle velocity u_p^2 is proportional to η^3. Results shown later in this paper tend to favor an ignition rate dependence of $r=3$ or greater.

An alternate model of hot-spot formation is based on the amount of plastic work required at void peripheries for dynamic void collapse. This mechanism was originally suggested by Taylor and discussed in later papers by Wackerle.[16,21] It predicts that the amount of plastic work required for hot-spot formation due to void collapse depends on the pressure and its application rate and is proportional to $\int p^2\,dt$. To investigate the p^2 ignition dependence, Eq. (2) with $r=4$ is used in the ignition and growth calculations and yields the best overall agreement with experiment as shown in Sec. III.

C. Growth of reaction from ignited hot spots

The second term in Eq. (2), which describes the growth of the reaction, is the most physically justifiable one of several that were formulated. The constant G corresponds to a surface area to volume ratio and the p^z term represents a pressure dependent laminar burn rate. The pressure exponents measured for laminar deflagration rates in explosives are generally on the order of 0.8–1.0 for pressures below 0.1 GPa.[52] There is some experimental evidence that an abrupt increase in the pressure exponent to approximately 2.0 occurs at higher pressures.[53] However, there is also experimental evidence that large increases in burning surface area are the principal cause of the rate increases in closed bomb tests on nitramine-based propellants above 0.2 GPa.[54] We will illustrate two approaches to the growth process. We will either fix the exponent z at 1.0 to specifically show the degree to which the burning surface area must increase or we will fix z at the smallest value that yields good agreement with shock initiation data. In both cases the sustained shock pulse experiments will be used for parameterization. The steepness of the run distance to detonation versus shock pressure data, especially for TATB-based ex-

plosives,[55] indicates a strong pressure and/or surface area dependence for the growth of reaction. The $(1-F)^x F^y$ term in the growth reaction rate forces the rate to zero when F equals zero and one, but also determines the geometry of the hot spots and the value of F at which their growth rate maximizes. Since spherical hot spots are implied by the various concepts of their formation and ignition, the constant y is set equal to $\frac{2}{3}$, since $F^{2/3}$ corresponds to the surface area of spherical hot spot burning outward.[24] The maximum of $(1-F)^x F^y$ occurs at $F=y/(x+y)$. A value of x equal to $\frac{2}{9}$ is used in Eq. (2) to maximize $(1-F)^x F^y$ at $F=\frac{3}{4}$, which corresponds to the maximum relative volume that uniform size spheres can occupy. The $(1-F)^{2/9}F^{2/3}$ term has little affect at small values of F but does affect the completion of reaction as $F \to 1$. Relatively rapid transitions from shock initiation to detonation and steady-state detonation reaction zone lengths in good agreement with experiment values are obtained in ignition and growth calculations that used $(1-F)^{2/9}F^{2/3}$. This section has described the reasoning behind the choices of parameters in the ignition and growth models. In the next section, detailed comparisons of various model calculations with experimental one-dimensional shock initiation data are presented to illustrate how the parameters r and z in Eq. (2) affect the calculational predictions.

III. COMPARISON OF EXPERIMENTAL AND CALCULATED RESULTS

A. General trends in the calculations

One-dimensional hydrodynamic calculations of shock initiation based on various forms of the ignition and growth reaction rate equation are compared with experimentally measured pressure or particle velocity histories at various embedded gage positions in the explosive. Sustained and short duration shock pulse and wedge test run distance to detonation versus shock pressure dependences are compared for PBX-9404, TATB, cast and pressed TNT, and PETN at densities near theoretical maximum density. Run distance to detonation versus shock pressure data for PETN at four initial densities from 1.0 g/cm^3 to 1.75 g/cm^3 are also used to compare the various models. Good overall agreement between the ignition and growth calculations and the experimental records is obtained for the two reaction rate equations,

$$\frac{\partial F}{\partial t}=I(1-F)^{2/9}\eta^4+G(1-F)^{2/9}F^{2/3}p^z, \tag{5}$$

where z is between 1.2 and 2.0 for the four explosives, and

$$\frac{\partial F}{\partial t}=I(1-F)^{2/9}\eta^4+G(p_i)(1-F)^{2/9}F^{2/9}p^{1.0}, \tag{6}$$

where the pressure exponent is 1.0 and the growth coefficient $G(P_i)$ increases as the input shock pressure p_i increases. The η^4 (or p^2) dependence of the ignition term is effective in predicting the differences in the amplitude increase of the leading shock front measured at several manganin gage positions as a function of initial shock pressure and the differences in initiation behavior as a function of initial density. Ignition and growth calculations based on η^3 (or u_p^2) are nearly as successful as those based on η^4.

Manganin pressure gage records and the run distance to detonation at a particular input pressure can be matched fairly well with a pressure exponent of 1.0 and a fixed value of G. However, when other input pressures are calculated, the calculated run-distance shock-pressure curves are not nearly as steep as the experimental results. In the ignition and growth calculations, the ignition term burns a very small fraction of explosive, which is always less than the original available void volume during shock compression. The ignition term is turned off when the shock compression is complete and the artificial viscosity approaches zero. The growth term then dominates the reactive flow. The detailed gage records and run distance to detonation curves are calculated in two ways illustrated by Eqs. (5) and (6). In Eq. (5), a value of z is chosen that gives good agreement with the detailed shapes of gage data and the run distance data. The values of I, G, and z used for the four explosives studied are listed in Table III. Equation (6) demonstrates the dependence of the growth term on the ignited surface area as a function of input shock pressure p_i required to match the experimental data for a pressure exponent of 1.0. Table IV contains values of I and $G(p_i)$ that gave good agreement with gage buildup and run distance to detonation data for these four heterogeneous explosives and shows that factor of six or smaller changes in $G(p_i)$ can match the observed steepness of run distance to detonation data.

B. Results for sustained shocks in high density explosives

Equation (5), with the values listed in Table III, currently yields the best overall agreement with the detailed shapes of embedded gage records and run distance to detonation data, and is used for comparison with experimental data in this paper. Figure 1 shows the calculated and experimental manganin gage pressure histories in PBX 9404 at several gage locations for a sustained shock pulse of 2.5 GPa.[20] Ignition and growth calculations are also in close agreement with the sustained pulse manganin gage records of Wackerle *et al.*[21] in PBX 9404 at 3.0 GPa. Figure 2 shows the calculated and VISAR measured particle velocity histories at the explosive/fused silica interface for 3.7 GPa, 1.1-μsec shock pulse in PBX-9404.[14] The difference

TABLE III. Ignition and growth reaction rate parameters for Eq. (5).

Explosive	PBX-9404	TATB	PETN	Cast TNT
$I(\mu\text{sec}^{-1})$	44	50	20	50
$G(\mu\text{sec}^{-1}\ \text{Mbars}^{-Z})$	200 [a]	125	400	40
Z	1.6	2.0	1.4	1.2

[a] Extrapolating the laminar burn rates measured for HMX below 0.2 GPa by Boggs *et al.* (Ref. 54) to 2.5 GPa, this value of G yields a surface area/volume ratio of 215 cm^{-1} for the growth of reaction in shock initiated PBX-9404.

TABLE IV. Ignition and growth rate parameters for Eq. (6).

Explosive	PBX-9404	TATB	PETN	Cast TNT
$I(\mu sec^{-1})$	44	50	20	50
$G(P_i)$	(μsec^{-1} $Mbars^{-1}$) $G(P_i = 2.5\ GPa) = 38$ [b] $G(P_i = 3\ GPa) = 44$ $G(P_i = 5\ GPa) = 75$ $G(P_i = 7.5\ GPa) = 130$ $G(P_i = 10\ GPa) = 176$	$G(P_i = 10.8\ GPa) = 15$ $G(P_i = 11.6\ GPa) = 24$ $G(P_i = 15\ GPa) = 45$ $G(P_i = 20\ GPa) = 90$	$G(1.5\ GPa) = 80$ $G(1.9\ GPa) = 100$ $G(2.7\ GPa) = 200$ $G(3.2\ GPa) = 250$	a

[a] No experimental run distance to detonation versus shock pressure data available for this particular cast TNT ($\rho = 1.61\ g/cm^3$).

[b] Extrapolating the laminar burn rates measured for HMX below 0.2 GPa by Boggs *et al.* (Ref. 54) to 2.5 GPa, this value of $G(P_i = 2.5\ GPa)$ yields a surface area/volume ratio of 374 cm^{-1} for the growth of reaction in shock initiated PBX-9404.

between the experimental and calculated records at 6 mm in Fig. 2 may be due to the overtaking of the shock front by the reactive pressure pulse in the 1.5-mm thick buffer placed behind the explosive in the VISAR experiments. In each of these studies, the leading shock front is observed to slowly increase in amplitude, but the main growth of reaction occurs behind the front. The ignition and growth calculations agree quite closely with the manganin gage records until the gages fail in the rapid pressure buildup region which precedes transition to detonation.

In the first reported manganin gage study of shock initiation,[16] PETN at a density of 1.75 g/cm^3 built up to detonation in a manner very similar to PBX-9404. Figure 3 shows the calculated and experimental pressure histories for a sustained, 1.9-GPa shock pulse in PETN. Again, the agreement between calculated and experimental records is good up to the pressure at which the gages fail, and the calculated run distance to detonation also agrees with experiment.

Manganin gage records in sustained pulse initiation of cast TNT[17,18] and TATB[20] appear to be quite different from those in PBX-9404 and PETN, since the leading shock front increases in amplitude more rapidly and the growth of reaction occurs closer to the front. In the ignition and growth calculations, the higher-shock pressures required for shock initiation of cast TNT and TATB cause larger fractions of the explosives to be ignited and correspondingly earlier increases in the growth of reaction. From this point of view, it is merely the increased relative importance of ignition to growth that created the differently shaped pressure histories. In fact, a change from PBX-9404-like to TATB-like pressure hisotries is sometime predicted in ignition and growth calculations simply as the input pressure is increased. Figure 4 shows the calculated and experimental pressure histories at several manganin gage locations for a sustained pulse initiation of cast TNT at 6.5 GPa.[17] Figure 5 shows the calculated and experimental pressure histories in TATB (actually RX-03-BB) subjected to a 11.6 GPa sustained shock pulse.[20]

Thus, the ignition and growth model based on Eq. (5) and the values in Table III has successfully calculated all of the sustained pulse manganin pressure gage and particle velocity measurement data for four solid explosives at densities near their theoretical maximum densities. Figure 6 shows the calculated and experimental run distance to detonation versus input shock pressure curves[3,16,56] for these four explosives. The experimental curve for this particular cast TNT (ρ_0

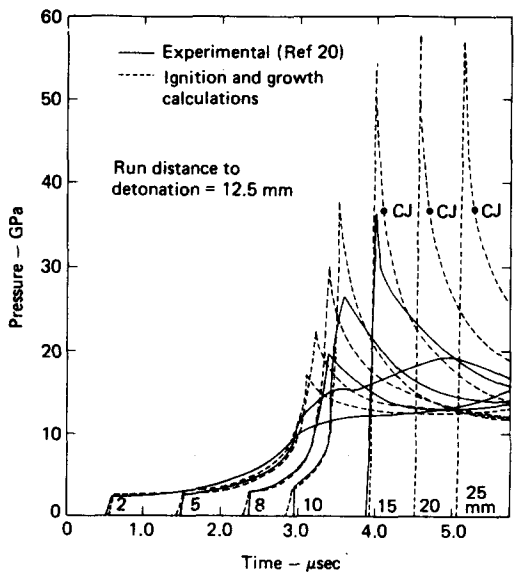

FIG. 1. Calculated and experimental pressure histories for a sustained shock pulse of 2.5 GPa in PBX-9404.

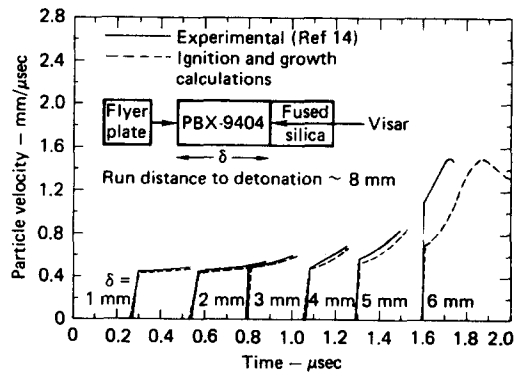

FIG. 2. Calculated and experimental particle velocity histories for 3.7 GPa, 1.1 μsec shocks in PBX-9404.

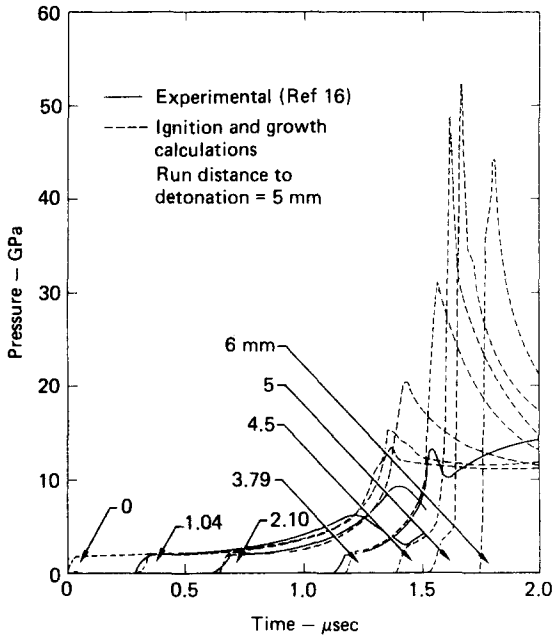

FIG. 3. Calculated and experimental pressure histories for a sustained shock pulse of 1.9 GPa in PETN.

$=1.61$ g/cm^3) is not available. Also shown in Fig. 6 are two calculated curves for PBX-9404 using a pressure exponent of 1.0: one which used $G(p_i)$ data listed in Table IV and one which used the value of $G(p_i = 2.5$ GPa), for all input pressures to demonstrate the necessity of a higher pressure exponent, or an increase in surface area with increasing shock pressure. Again, the good agreement with run-distance data lends support for the phenomenological rationale of the ignition and growth models.

C. Sustained shocks in porous explosives

One set of manganin gage data has been published for an explosive with a moderate degree of porosity (TNT

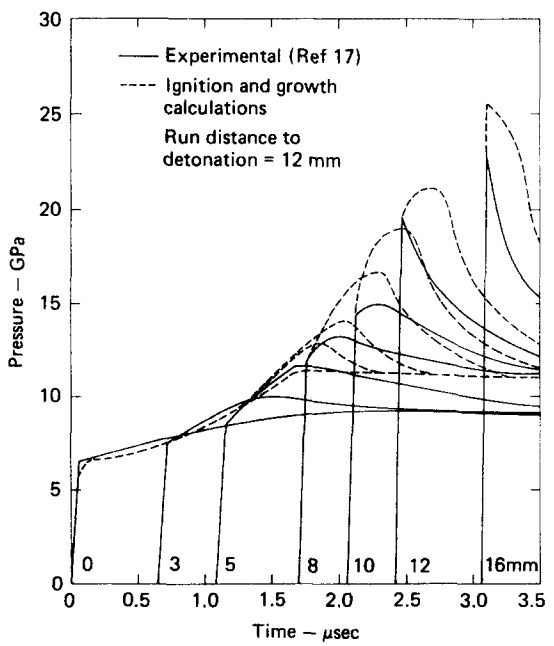

FIG. 4. Calculated and experimental pressure histories for a sustained shock pulse of 6.5 GPa in cast TNT.

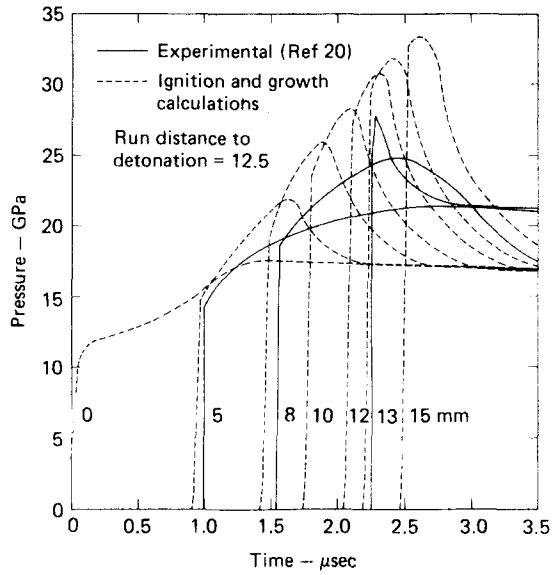

FIG. 5. Calculated and experimental pressure histories for a sustained shock pulse of 11.6 GPa in TATB (RX-03-BB).

pressed to 1.56 g/cm^3).[19] Figure 7 shows the calculated and experimental pressure histories for TNT pressed to 1.56 g/cm^3 and shocked to approximately 4 GPa. Since Belinets, *et al.*[19] used the same unreacted Hugoniot for pressed and cast TNT, the calculations in Fig. 7 used the TNT values listed in Tables I, II, and III, with the initial density, initial energy and heat of reaction reduced by the appropriate initial density factor. The slightly more porous pressed TNT exhibited significantly more ignition and shock front growth than cast TNT, and the ignition and growth calculations predict this increased ignition.

A more severe test of the model for porous explosives is the run distance to detonation versus shock pressure data for PETN[2,4,16] at four initial densities: 1.0, 1.6, 1.72, and 1.75 g/cm^3. Jones–Wilkins–Lee equations of state were formulated for the unreacted PETN at 1.0, 1.6, and 1.72 g/cm^3, based on the available sound vel-

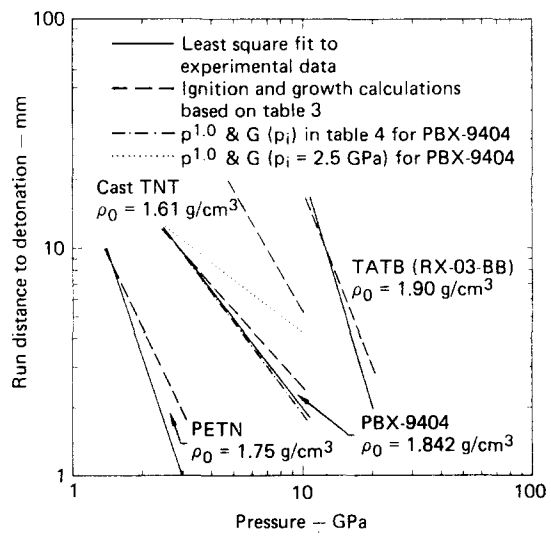

FIG. 6. Calculated and experimental run distance to detonation versus shock pressure data for sustained pulses.

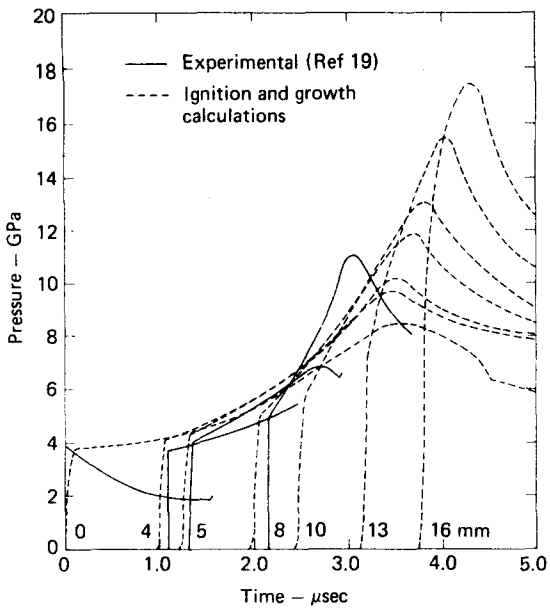

FIG. 7. Calculated and experimental pressure histories for a sustained shock pulse of 4 GPa in TNT pressed to 1.56 g/cm^3.

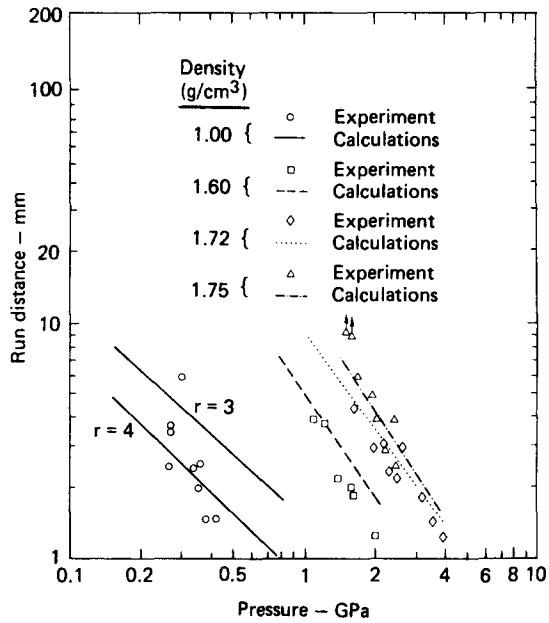

FIG. 8. Calculated and experimental run distance to detonation versus shock pressure curves for PETN at various initial densities.

ocity, shock velocity and particle velocity data.[2,4] Fits to cylinder test data were already available for the reaction products of PETN at various densities.[45] Table V contains the parameters used for unreacted PETN and its reaction products at the three lower densities. Figure 8 shows the experimental run distance to detonation data for PETN and the calculated run-distance curve for each density using the appropriate equations of state and the reaction rate values listed in Table III. Also shown in Fig. 8 is a curve marked $r=3$ which represents the run distances for 1.0 g/cm^3 PETN calculated using $r=3$ in Eq. (2) and the values of I, G, and z that gave the best agreement with manganin gage data for 1.75 g/cm^3 PETN. There is a great deal of uncertainty in the unreacted Hugoniot of 1.0-g/cm^3 PETN and in the resulting pressures attributed to flyer plate impact of this porous explosive, but the $r=3$ and $r=4$ calculations bracket the experimental run distances. The ignition and growth model, normalized to manganin gage and run distance data for high-density explosives, yields a reasonable prediction of the shock initiation properties of the same explosives pressed to lower initial densities.

TABLE V. Equation of state parameters for low density PETN.

	Unreacted explosive		
ρ_0(g/cm^3)	1.72	1.60	1.00
A(Mbars)	346.6	21.88	13.12
B(Mbars)	−3.3	−0.58	−0.078 4
R_1	10.0	7.8	11.0
R_2	5.0	3.9	5.5
w	0.755 6	0.3468	0.020 27
Cv(Mbars/°K)	2.887×10^{-5}	2.685×10^{-5}	$1.676\,6\times10^{-5}$
	Reaction products		
A(Mbars)	6.17	6.253	2.372
B(Mbars)	0.169 26	0.2329	0.106 1
R_1	4.4	5.25	5.6
R_2	1.2	1.6	1.8
w	0.25	0.28	0.24
Cv(Mbars/°K)	1×10^{-5}	1×10^{-5}	1×10^{-5}
E_0(Mbars-cc/cc)	0.098 15	0.0913	0.057 06

D. Results for short pulse duration shock initiation

The final type of available shock initiation data to which ignition and growth calculations can be compared is the short pulse duration data. Manganin gage data on short pulse initiation is available for cast TNT[18] and

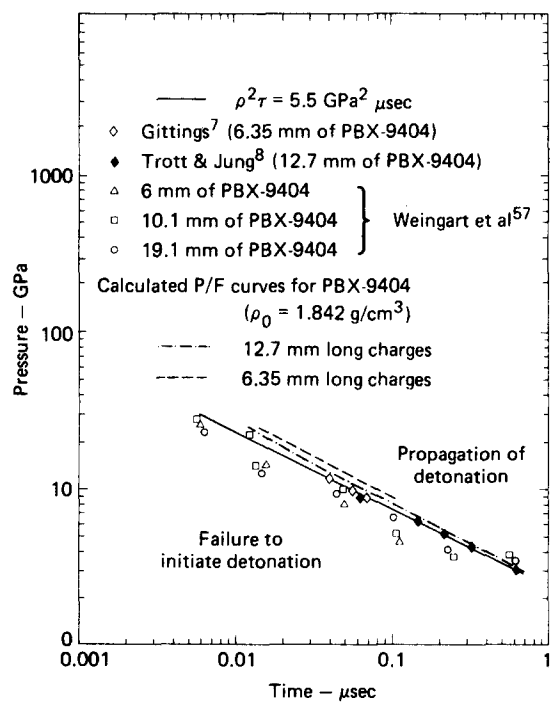

FIG. 9. Calculated and experimental propagation/failure curves of pressure versus pulse duration in PBX-9404.

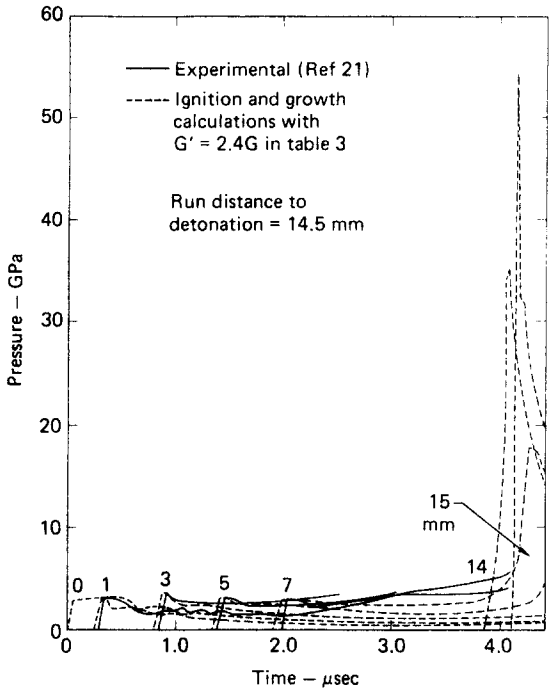

FIG. 10. Calculated and experimental pressure histories for a 3-GPa, 0.33-μsec shock in PBX-9404.

PBX-9404.[21] A great deal of propagation/failure (P/F) and excess transit time data for short duration pulses in various charge lengths of PBX-9404 is contained in the works of Gittings[7] and Trott and Jung.[8] Recently, Weingart *et al.*[57] using electrically driven thin plastic flyer plates obtained P/F data at high pressures approaching 28 GPa and very short pulse durations approaching 7 nsec. When applied to this short pulse duration data for PBX-9404, the ignition and growth model gives good agreement with P/F pressure-pulse duration experiments and the $p^2\tau$ criterion, as shown in Fig. 9. When compared to the manganin gage records in both PBX-9404 and cast TNT, the calculated growth of pressure behind the shock front is slightly slow and the run distances to detonation are slightly too long. Increasing the growth coefficient G in Table III by a factor of 2.4 for PBX-9404 and 2.5 for cast TNT, yields the improved pressure histories shown in Figs. 10 and 11 for a 3 GPa, 0.33-μsec shock pulse in PBX-9404 and a 8.5 GPa, 0.25-μsec pulse in cast TNT, respectively. This improved agreement with higher values of G may indicate that a process is occurring which increases the available surface area for ignition as the rarefaction wave, which follows the short duration shock pulse, interacts with the reacting hot-spot sites.

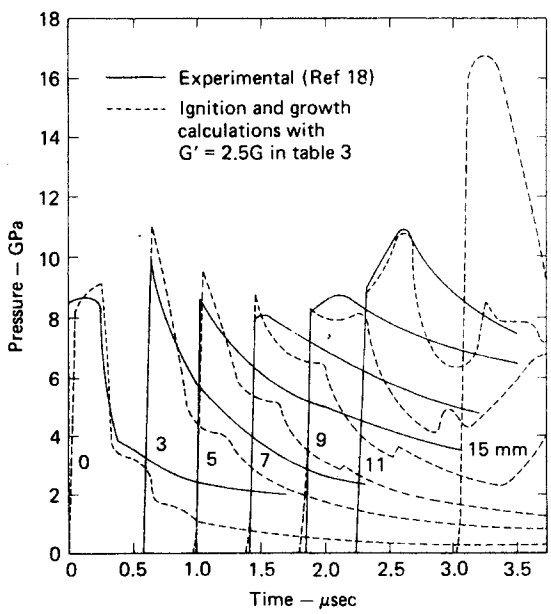

FIG. 11. Calculated and experimental pressure histories for a 8.5-GPa, 0.25-μsec shock in cast TNT.

IV. CONCLUSIONS

Application of the ignition and growth concept of shock initiation through one-dimensional hydrodynamic computer modeling to the published experimental pressure-time, particle velocity-time, and run distance to detonation data, has led to the following conclusions:

(1) The fraction of the explosive that must be ignited in the hydrodynamically created hot spots is well below the initial void volume fraction that would be collapsed during shock compression.

(2) Ignition models, based on either the stagnation of material during void collapse or plastic work during void closure to produce hot spots, yield good agreement with experimental data. Hot-spot ignition must involve a complex combination of mechanisms which generate and dissipate thermal energy. A two-dimensional hydrodynamic study of the thermodynamic conditions reached in dynamic void closure in PBX-9404 is currently underway.[58]

(3) The growth of reaction from these ignition sites apparently proceeds at rates that exceed the linear burn rate-pressure dependence of laminar deflagration in explosives. The growth of reaction can be accurately modeled using a higher pressure dependence and/or a surface area/volume ratio that gradually increases with increasing input shock pressure. Threshold conditions for ignition and growth of smaller hot spots being attained as the shock pressure increases should be considered as a probable phenomenon.

(4) By using the ignition and growth parameters developed for the maximum pressing density of a particular explosive, the experimental shock initiation results for explosives pressed to initial densities significantly lower than theoretical can be predicted to within the uncertainty in the hydrodynamic properties of the porous explosives. Only the equations of state of the porous explosive and its reaction products were adjusted to match experimental data.

(5) The short pulse duration shock initiation data on PBX-9404 can also be predicted by the sustained pulse ignition and growth models. Improved quantitative agreement with manganin pressure gage data in short pulse initiations of PBX-9404 and cast TNT is obtained using an increased surface area/volume for reactive growth.

(6) Further development of this phenomenological

shock initiation concept will require more detailed information on the constitutive properties of unreacted explosives, since hot-spot formation and subsequent ignition are strongly dependent on the transformation of shock energy into localized heating. Further experimental work on laminar burn rates at high pressures would be very useful tests of the validity of the model. Our results indicate major differences in these rates for PETN and PBX-9404 on the one hand and TATB on the other, TATB exhibiting the smaller rate. However, we can estimate surface-to-volume ratios for growth of reaction sites only in PBX-9404, because we lack high pressure burn rate data for other explosive materials.

(7) Since the ignition and growth models have been successful in predicting one-dimensional initiation and detonation properties, a two-dimensional hydrodynamic computer study of shock initiation tests, detonation wave front curvature, failure diameter, corner-turning, and other two-dimensional effects in heterogeneous explosives is currently underway.

ACKNOWLEDGMENTS

We would like to thank S. G. Cochran of Lawrence Livermore National Laboratory for providing us with his special version of KOVEC and for many interesting discussions. We would like to thank H. Cheung and E. Kahara of Lawrence Livermore National Laboratory for incorporating the equations of state and ignition and growth models into this KOVEC version. Discussions with the following scientists greatly increased our knowledge of shock initiation experiments and theory: L. Erickson, L. Green, R. McGuire, W. Von Holle, and F. Walker of Lawrence Livermore National Laboratory; M. Cowperthwaite of SRI International; J. Kennedy and J. Nunziato of Sandia Corporation; C. Forest, M. Ginsberg, and J. Wackerle of Los Alamos Scientific Laboratory; J. Enig of Naval Surface Weapons Center; and A. N. Dremin of the U.S.S.R.

This work was performed under the auspices of the U.S. Department of Energy by the Lawrence Livermore National Laboratory under Contract No. W-7405-Eng-48.

[1]A. W. Campbell, W. C. Davis, J. B. Ramsey, and J. R. Travis Travis, Phys. Fluids **4**, 511 (1961).
[2]G. E. Seay and L. B. Seely, Jr. J. Appl. Phys. **32**, 1092 (1961).
[3]J. B. Ramsey and A. Popolato, in *Fourth Symposium (International) on Detonation*, ACR-126 (Office of Naval Research, Washington, D. C., 1965), p. 233.
[4]D. Stripe, J. O. Johnson, and J. Wackerle, J. Appl. Phys. **41**, 3884 (1970).
[5]I. E. Lindstrom, J. Appl. Phys. **37**, 4873 (1966).
[6]I. E. Lindstrom, J. Appl. Phys. **41**, 337 (1970).
[7]E. F. Gittings in *Fourth Symposium (International) on Detonation*, ACR-126 (Office of Naval Research, Washington, D. C., 1965), p. 373.
[8]B. D. Trott and R. G. Jung, in *Fifth Symposium (International) on Detonation*, ACR-184 (Office of Naval Research, Pasadena, Calif., 1970), p. 191.
[9]T. P. Liddiard, Jr., in *Fourth Symposium (International) on Detonation*, ACR-126 (Office of Naval Research, Washington, D.C., 1965), p. 487.
[10]L. Green (private communication).
[11]B. G. Craig and E. F. Marshall, in *Fifth Symposium (International) on Detonation*, ACR-184 (Office of Naval Research, Pasadena, Calif., 1970), p. 321.
[12]J. E. Kennedy, in *Fifth Symposium (International) on Detonation*, ACR-184 (Office of Naval Research, Pasadena, Calif., 1970), p. 435.
[13]J. E. Kennedy, in *Fourteenth Symposium (International) on Combustion* (The Combustion Institute, Pittsburgh, Pa., 1972), p. 1251.
[14]J. E. Kennedy and J. W. Nunziato, J. Mech. Phys. Solids **24**, 107 (1976).
[15]M. Cowperthwaite and J. T. Rosenberg, in *Sixth Symposium (International) on Detonation*, ACR-221 (Office of Naval Research, Coronado, Calif., 1976), p. 786.
[16]J. Wackerle, J. O. Johnson, and P. M. Halleck, in *Sixth Symposium (International) on Detonation*, ACR-221 (Office of Naval Research, Coronado, Calif., 1976), p. 20.
[17]G. I. Kanel and A. N. Dremin, Combust. Explos. Shock Waves (USSR) **13**, 71 (1977).
[18]G. I. Kanel, Combust. Explos. Shock Waves (USSR) **14**, 92 (1978).
[19]Yu. M. Belinets, A. N. Dremin, and G. I. Kanel, Combust. Explos. Shock Waves (USSR) **14**, 361 (1978).
[20]R. Weingart, R. Barlett, S. Cochran, L. Erickson, J. Chan, J. Janzen, R. Lee, D. Logan, and J. T. Rosenberg, in *Proceedings of the Symposium on High Dynamic Pressures* (Commissariat á l'Energie Atomique Paris, France, 1978), p. 451.
[21]J. Wackerle, R. L. Rabie, M. J. Ginsberg, and A. B. Anderson, in *Proceedings of the Symposium on High Dynamic Pressures* (Commissariat à l'Energie Atomique Paris, France, 1978), p. 127.
[22]L. Green, E. Nidick, E. Lee, and C. Tarver, in *Proceedings of the Symposium on High Dynamic Pressures* (Commissariat à l'Energie Atomique Paris, France, 1978), p. 115.
[23]F. P. Bowden and A. D. Yoffe, *Initiation and Growth of Explosives in Liquids and Solids* (Cambridge University, Cambridge, Massachusetts, 1952).
[24]H. Eyring, R. E. Powell, G. H. Duffrey, and R. B. Darlin, Chem. Rev. **45**, 69 (1949).
[25]H. W. Hubbard and M. H. Johnson, J. Appl. Phys. **30**, 765 (1959).
[26]C. L. Mader, Phys. Fluids **6**, 375 (1963).
[27]C. L. Mader, Phys. Fluids **8**, 1811 (1965).
[28]M. H. Boyer, J. Appl. Phys. **40**, 654 (1969).
[29]J. W. Enig and F. J. Petrone, Phys. Fluids **9**, 398 (1966).
[30]F. J. Petrone, Phys. Fluids **11**, 1473 (1968).
[31]M. Cowperthwaite and R. Shaw, J. Chem. Phys. **53**, 555 (1970).
[32]F. E. Walker and R. J. Wasley, Explosivestoffe **17**, 9 (1969).
[33]Discussion on Shock Initiation and $p^2\tau$, in *Sixth Symposium (International) on Detonation*, ACR-221 (Office of Naval Research, Coronado, Calif., 1976), p. 82.
[34]Y. de Longueville, C. Fauguignon, and H. Moulard, in *Sixth Symposium (International) on Detonation*, ACR-221, (Office of Naval Research, Coronado, 1976), p. 105.
[35]H. Bernier, A. Vidart, and F. Prouteau, presented at the International Conference on Sensitivity and Hazards of Explosives, London, England, October 1963.
[36]C. L. Mader and C. A. Forest, Los Alamos Scientific Laboratory Report LA-6259 (1976).
[37]C. L. Mader, in *Sixth Symposium (International) on Detonation*, ACR-221 (Office of Naval Research, Coronado, 1976), p. 405.
[38]C. A. Forest, Los Alamos Scientific Laboratory Report LA-7245, 1978.
[39]M. Cowperthwaite, in *Proceedings of the Symposium on High Dynamic Pressures* (Commissariat à l'Energie Atomi-

que, Paris, France, 1978), p. 201.
[40]J. W. Nunziato, E. K. Walsh, and J. E. Kennedy, in *Proceedings of the Symposium on High Dynamic Pressures* (Commissariat à l'Energie Atomique Paris, France, 1978), p. 139.
[41]E. L. Lee, H. Cheung, and C. M. Tarver, Bull. Am. Phys. Soc. 23, 36 (1978).
[42]S. G. Cochran and J. Chan, Lawrence Livermore Laboratory Report UCID-18024, 1978.
[43]Y. B. Zeldovich and A. S. Kompaneets, *Theory of Detonation* (Academic, New York, 1960), Chap. 2.
[44]E. L. Lee, H. C. Hornig, and J. W. Kury, Lawrence Livermore Laboratory Report UCRL-50422, 1968.
[45]E. Lee, M. Finger, and W. Collins, Lawrence Livermore Laboratory Report UCID-16189, 1973.
[46]B. C. Taylor and L. H. Ervin, in *Sixth Symposium (International) on Detonation*, ACR-221 (Office of Naval Research, Coronado, Calif.,1976), p. 3.
[47]W. G. Von Holle, in *Proceedings of the Symposium on High Dynamic Pressures* (Commissariat à l'Energie Atomique Paris, France, 1978), p. 425.
[48]P. Howe, R. Frey, B. Taylor and V. Boyle, in *Sixth Symposium (International) on Detonation*, ACR-221 (Office of Naval Research, Coronado, Calif.,1976), p. 11.
[49]L. B. Seely, in *Proceedings of the Fourth Electric Initiator Symposium* (Franklin Institute, Philadelphia, Pa.,1963), paper 27.
[50]R. H. Stresau and J. E. Kennedy, in *Sixth Symposium (International) on Detonation*, ACR-221 (Office of Naval Research, Coronado, Calif., 1976), p. 68.
[51]J. Roth, in *Fifth Symposium (International) on Detonation*, ACR-184 (Office of Naval Research, Pasadena, Calif.,1970), p. 219.
[52]K. K. Andreev and S. V. Chniko, Russian J. Phys. Chem. 37, 695 (1963).
[53]N. S. Cohen (private communication).
[54]T. L. Boggs (private communication).
[55]R. K. Jackson, L. G. Green, R. H. Bartlett, W. W. Hofer, P. E. Kramer, R. S. Lee, E. J. Nidick, Jr., L. L. Shaw, and R. C. Weingart, in *Sixth Symposium (International) on Detonation*, ACR-221 (Office of Naval Research, Coronado, 1976), p. 755.
[56]L. G. Green, E. J. Nidick, Jr., and F. E. Walker, Lawrence Livermore Laboratory Report UCRL-51522, 1974.
[57]R. C. Weingart, R. K. Jackson, C. A. Honodel, and R. S. Lee, presented at the Tenth Symposium on Explosives and Pyrotechnics, Franklin Institute, San Francisco, Calif., 1979.
[58]J. Walton (private communication).